Exploring the ages of rotating stars using galactic dynamics: a novel approach to calibrating gyrochronology

Ruth Angus *et al.*

ABSTRACT

The rotational evolution of cool dwarfs is poorly constrained after ∼2-3 billion years due to a lack of precise ages and rotation periods for old main-sequence stars. In this work, we use the velocities of low-mass *Kepler* dwarfs to reveal their rotational evolution and demonstrate that kinematics have potential to be a useful tool for calibrating gyrochronology. At ages less than ∼1 Gyr we find that a gyrochronology model, calibrated to the Praesepe cluster, accurately predicts the relative ages of stars. At these young ages, lower-mass stars lose angular momentum more quickly than higher mass stars and therefore rotate more slowly at the same age. However, at old ages, late G and early K dwarfs rotate *faster* than late K dwarfs of the same age. This implies that low-mass stars lose angular momentum more slowly than higher-mass stars after a certain age or Rossby number. Our results, based on field star rotation periods, align with recent findings from the rotation periods of stars in middle-aged open clusters and theoretical models that vary the rate of surface-to-core angular momentum transport. Finally, we find no evidence for mass-dependent heating in a sample of K and M dwarfs in the *Kepler* field.

1. Introduction

1.1. Gyrochronology

It is well established that the rotation periods of FGKM dwarfs increase over time (*e.g.* **????**Barnes 2003, 2007; **?**; Meibom et al. 2011; **?**), however the exact nature and form of rotational evolution is still being actively studied. In particular, as new rotation period measurements for stars with precise ages become available, the mass-dependence of the relationship between rotation and age appears to be more complicated than once thought. From both observations and theoretical modelling, stars of different masses are expected to have different rotation periods (*e.g.* ??), which is thought to be mainly driven by variation in convection zone depth. For example in the Praesepe cluster, M dwarfs spin more slowly than G dwarfs, presumably because lower mass stars with deeper convections zones are have stronger magnetic dynamos and lose angular momentum more rapidly. However, new rotation period measurements show that variation in convection zone depth cannot be solely responsible for mass-dependent rotational evolution. For example, old field stars seem rotate more rapidly than models predicted (Angus et al. 2015; van Saders et al. 2016, 2018; Metcalfe and Egeland 2019), and a mass-dependent modification to the classical $P_{\rm rot} \propto t^{\frac{1}{2}}$ spin-down law (Skumanich 1972) is required to reproduce the data (van Saders et al. 2016, 2018). Recent analyses of the 1.1 Gyr open cluster, NGC 6811, provide further indication that the exponent of the period-age relation is mass and time-dependent (?). This cluster has a flattened relationship between rotation period and color: the G dwarfs rotate at the same rate as the K dwarfs. New semi-empirical models that vary the redistribution of angular momentum in the interiors of stars are able to reproduce this flattened period-color relation (?). We now know that the rotational evolution of stars is a complicated process, however relying on open clusters (which are typically young) and asteroseismic stars (which are typically G-type stars or more massive) to calibrate gyrochronology relations limits the mass and age coverage of the calibration sample. In this paper, we use stellar velocity dispersions to gain insight into the rotational evolution of field stars. This technique provides relative ages for groups of stars that cover a broad range of masses and ages, allowing us to observe the rotational evolution of stars in an average sense.

1.2. Kinematics as an age proxy

Stars are thought to be born in the thin disk of the Milky Way (MW), orbiting the galaxy with a low out-of-plane, or vertical, velocity (W, or $v_{\mathbf{z}}$), just like the star-forming molecular gas observed in the disk today (*e.g.* ??Aumer and Binney 2009; ?; Aumer et al. 2016). On average, the vertical velocities of stars increase over time (*e.g.* Nordström et al. 2004; Holmberg et al. 2007, 2009; Aumer and Binney 2009; ?). Although the cause of dynamical heating is not well understood, interactions with giant molecular clouds, spiral arms and the galactic bar are thought to play an important role (see Sellwood 2014, for a review of secular evolution in the MW). Although the velocity of any individual star will only provide a weak age constraint, the velocity dispersion of a group of stars can indicate whether, on average, that group is old or young relative to other groups. In this work we compare the velocity dispersions of groups of stars to ascertain which groups are older and which younger and draw conclusions based on the implied relative ages of populations.

Vertical velocity, $v_{\mathbf{z}}$, can only be calculated with full 6-dimensional position and velocity information, and unfortunately most stars with measured rotation periods do not have radial velocity (RV) measurements because they are relatively faint *Kepler* targets (∼11th-18th magnitudes). For this reason, we used velocity in the direction of galactic latitude, $v_{\mathbf{b}}$, to mimic $v_{\mathbf{z}}$. The *Kepler* field is positioned at low galactic latitude (b=∼5-20°), so $v_{\mathbf{b}}$ is a close (although imperfect – see section 3) approximation to $v_{\mathbf{z}}$. Because we use $v_{\mathbf{b}}$ rather than $v_{\mathbf{z}}$ it is difficult to directly compare gyrochronal ages with kinematic ones using an age-velocity dispersion relation (AVR). However, regardless of direction, velocity dispersion is expected to monotonically increase over time, and can therefore be used effectively to *rank* groups of stars by age.

This paper is laid out as follows: in section 2 we describe our sample selection process and the methods used to calculated stellar velocities. We also establish that $v_{\mathbf{b}}$ velocity dispersion, $\sigma_{v\mathbf{b}}$, can be used as an age proxy by demonstrating that neither mass-dependent heating nor the selection function is likely to have a strong affect on our sample. In section 3 we use stellar kinematics to investigate the relationship between rotation period, age and color/T_{eff} in the field. We show that the period-color relation of Praesepe is not applicable to old stars in section 3.1, and reveal the true shape of the period-color relations in section 3.2. We discuss a possible connection with the rotation period gap in section 4.1.

2. Method

2.1. The data

We used the publicly available *Kepler*-*Gaia* DR2 crossmatched catalog[1] to combine the McQuillan et al. (2014) catalog of stellar rotation periods, measured from *Kepler* light curves, with the *Gaia* DR2 catalog of parallaxes, proper motions and apparent magnitudes. Reddening and extinction from dust was calculated for each star using the Bayestar dust map implemented in the `dustmaps` *Python* package (M. Green 2018), and `astropy` (Astropy Collaboration et al. 2013). We estimated effective temperatures from dereddened *Gaia* $G_{BP} - G_{RP}$ color, using an 8th-order polynomial relation calibrated using .... stars ask Jason for details.

$$\mathrm{T_{eff}} = 8960 - 4802C + 1931C^2 - 2446C^3 + 2669C^4 - 1324C^5 + 301C^6 - 26C^7, \quad (1)$$

where C is *Gaia* $G_{BP} - G_{RP}$.

Visual binaries and subgiants were removed from the sample by applying cuts to the color-magnitude diagram (CMD), shown in figure 1. A 6th-order polynomial was fit to the main sequence and raised by 0.27 dex to approximate the division between single stars and visual binaries. All stars above this line were removed from the sample. Subgiants were also removed by eliminating stars brighter than 6th magnitude in *Gaia* G-band.

The `Pyia` (Price-Whelan 2018) and `astropy` (Astropy Collaboration et al. 2013; Price-Whelan et al. 2018) *Python* packages were used to calculate stellar velocities. `Pyia` calculates velocity samples from the full *Gaia* uncertainty covariance matrix via Monte Carlo sampling. It therefore not only incorporates uncertainties on the *Gaia* positions parallaxes and proper motions, it also accounts for the *covariance* between these properties. Stars with negative parallaxes, parallax signal-to-noise ratios less than 10, stars fainter than 16th magnitude, stars with absolute $v_\mathbf{b}$ uncertainties greater than 1 kms^{-1} and stars with galactic latitudes greater than 15° were removed from the sample. Because $v_\mathbf{b}$ is only a close approximation to $v_\mathbf{z}$ at low galactic latitudes, and because latitude is correlated with stellar mass (lower mass stars are older and tend to be preferentially located at high b, although this trends is greatly reduced for stars cooler than 5000 K), we found that excluding stars with $b > 15°$ reduced the number of $v_\mathbf{b}$ outliers at low stellar mass. 15° was found to be an adequate compromise between maintaining a close relationship between $v_\mathbf{b}$ and $v_\mathbf{z}$ and retaining a sample large enough to provide meaningful results. Reducing this cut to 10° resulted in a sample size too

[1] Available at gaia-kepler.fun

Fig. 1.— Dereddened MS *Kepler* stars with McQuillan et al. (2014) rotation periods on the *Gaia* CMD. We excluded visual binaries by removing stars above the dashed line. Points are colored by their gyrochronal age, according to the Angus et al. (2019) gyrochronology relation. A general age gradient is visible across the main sequence.

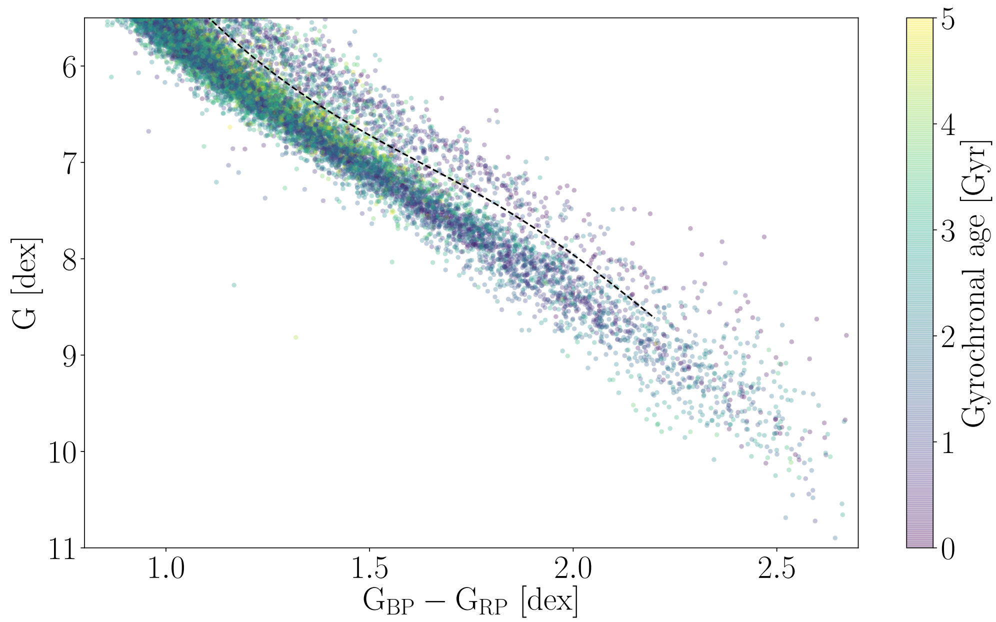

small to reveal trends in the data, and intermediate cuts did not significantly change the results.

2.2. Establishing $v_{\mathbf{b}}$ as an age proxy

If lower-mass stars experience greater velocity changes when gravitationally perturbed and are dynamically heated more efficiently than higher-mass stars, velocity dispersion would be a function of *both* age and mass and cannot be straightforwardly interpreted as an age proxy. So, in order to establish whether $\sigma_{v\mathbf{b}}$ can be used as an age proxy, we searched for signs of mass-dependent heating within the *Kepler* field.

Mass-dependent dynamical heating has not been unambiguously observed in the galactic disk because of the strong anti-correlation between stellar mass and stellar age. Less massive stars do indeed have larger velocity dispersions, however they are also older on average. This mass-age degeneracy is highly reduced in M dwarfs because their main-sequence lifetimes are longer than the age of the Universe, however no evidence for mass-dependent heating has been found in M dwarfs (Faherty et al. 2009; **?**).

To investigate whether mass-dependent heating could be acting on the *Kepler* sample, we selected late K and M dwarfs observed by both *Kepler* and *Gaia*, whose MS lifetimes exceed around 11 Gyrs and are therefore representative of the initial mass function. We could not perform this analysis on the McQuillan et al. (2014) sample, because only stars with *detectable* rotation periods appear there. Since lower-mass stars stay active for longer it is likely that there are more old stars (with larger velocity dispersions) at low masses in this sample. We selected all *Kepler* targets with dereddened *Gaia* $G_{BP} - G_{RP}$ colors greater than 1.2 (corresponding to an effective temperature $\lesssim$ 4800 K) and absolute *Gaia* G-band magnitudes < 4. We also eliminated visual binaries by removing stars above a 6th order polynomial, fit to the MS on the *Gaia* CMD. This polynomial-based binary cut was slightly different to the polynomial cut used... We then applied the quality cuts described in section 2.1. To search for evidence of mass-dependent heating we calculated the ($v_{\mathbf{b}}$) velocity dispersion of stars in effective temperature bins. Sigma clipping was performed at the 3σ level to remove high velocity outliers before calculating the standard deviation of stars in each bin.

Figure 2 shows velocity and velocity dispersion as a function of effective temperature (calculated by transforming dereddened *Gaia* colors using equation 1). Velocity dispersion very slightly *decreases* with decreasing temperature, the opposite of the trend expected for mass-dependent heating, however the slope is only inconsistent with zero at the 1.3 σ level.

This trend may be due to a selection bias: cooler stars are fainter and therefore typically closer, with smaller heights above the galactic plane and smaller velocities. The essential point is that we do not find evidence for mass-dependent heating acting on stars in the *Kepler* field, meaning $\sigma_{v\mathbf{b}}$ *can* be used as an age proxy. We performed the same analysis on the 537 stars in this sample with RVs using *vertical* velocity ($v_{\mathbf{z}}$) and found the slope of the velocity dispersion-temperature relation was consistent with zero.

Since we used $v_{\mathbf{b}}$, not $v_{\mathbf{z}}$ in our analysis, it is possible that an anti-correlation between $T_{\rm eff}$ and galactic latitude, b, could influence our results. Stars at higher latitudes have additional velocity components in the $\mathbf{x}$ and $\mathbf{y}$ directions, which could increase $v_{\mathbf{b}}$ but not $v_{\mathbf{z}}$. Again however, since the relationship between $\sigma_{v\mathbf{b}}$ and $T_{\rm eff}$ is positively, not negatively correlated for cool stars in the *Kepler* field, this effect is probably too small to influence our results.

Fig. 2.— Top: Stellar velocity ($v_{\mathbf{b}}$) as a function of T_{eff} for *Kepler* K and M dwarfs. Vertical lines indicate different T_{eff}-groupings used to calculate velocity dispersion. Pink stars were not included in velocity dispersion calculations as they were either removed as outliers during a sigma clipping process, or they lie at the sparcely populated, extremely cool end of the temperature range. Velocity dispersion and T_{eff} are slightly positively correlated, likely due to a brightness-related selection bias, indicating that mass-dependent heating does not significantly affect low-mass stars in the *Kepler* field.

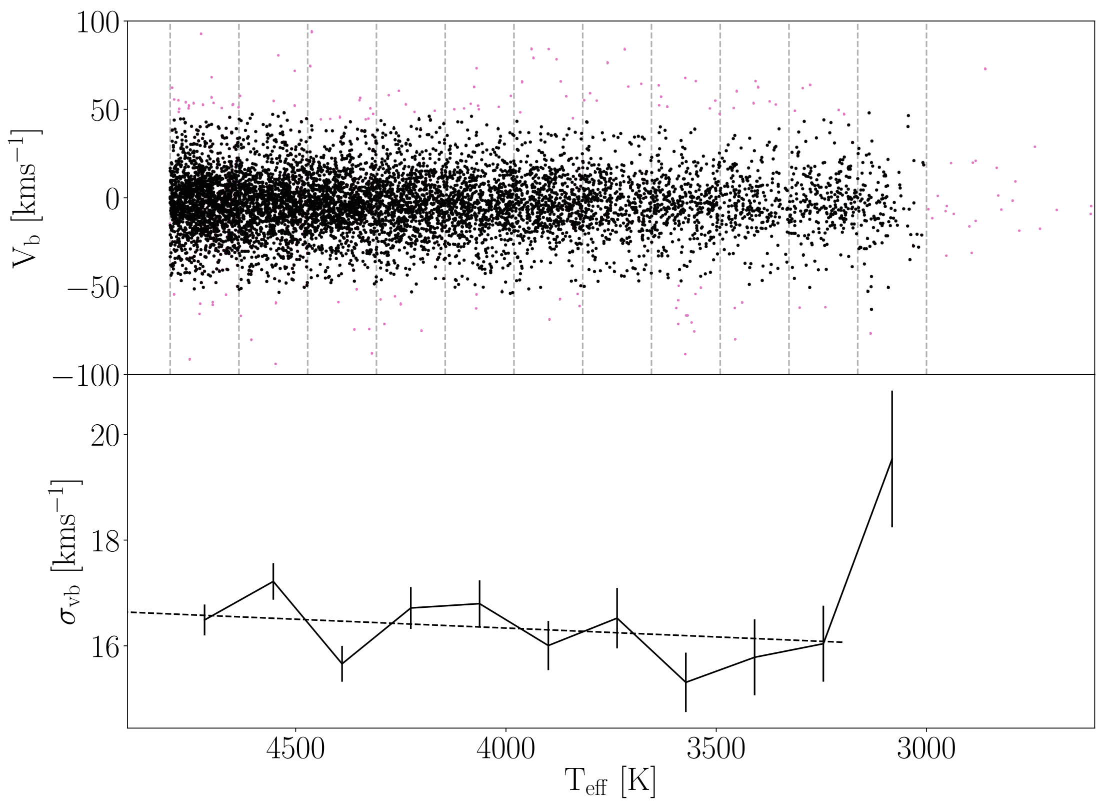

3. Results

3.1. Velocity dispersion of coeval groups

To explore the relationship between rotation period, T_{eff} and age for field K dwarfs, we calculated gyrochronal ages using dereddened (extinction was calculated using the M. Green 2018, Python package) *Gaia* photometry (G, G_{BP} and G_{RP}) and rotation periods from McQuillan et al. (2014). We used the Angus et al. (2019) gyrochronology relation which is a separable relation in $G_{BP} - G_{RP}$ color and age, calibrated using the period-color relation of Praesepe and the period-age relation of Praesepe and the Sun. The large number of Praesepe members with precise rotation periods from the *K2* mission (**?**Douglas et al. 2017; Rebull et al. 2017), spanning spectral types F through early M, makes it a good cluster for calibrating the period-color relation of stars at 650 Myrs. However, this is an extremely simple model and although it accurately describes the rotation periods of F and G stars up to around 2.5 Gyr (the age of NGC 6819 – the oldest cluster with available rotation periods), it over-predicts the rotation periods of K dwarfs in the 1.1 Gyr NGC 6811 cluster. These gyrochronal ages are shown on a *Gaia* color-magnitude diagram (CMD) in figure 1. The stars with old gyrochronal ages, plotted in yellow hues, predominantly lie along the upper edge of the MS, where stellar evolution models predict old stars to be, however the majority of these 'old' stars are bluer than $G_{BP} - G_{RP} \sim 1.5$ dex. This suggests that the Angus et al. (2019) gyrochronology relation under-predicts the ages of low-mass stars because there is no reason to expect the oldest stars in this sample to be the bluer ones: M dwarfs are, on average, older than K dwarfs and are expected to remain active for longer, so should therefore have measurable rotation periods at older ages.

To further explore the relationship between rotation period, T_{eff} and age, we selected groups of stars within different gyrochronal age ranges and calculated the velocity dispersion ($\sigma_{v\mathbf{b}}$), the standard deviation of $v_{\mathbf{b}}$ velocities, as a function of effective temperature for each age group. We performed 3σ sigma-clipping on the stellar velocities in each age and temperature bin to remove non-Gaussian outliers. Without sigma-clipping, we found that a small number of high velocity outliers at the low-temperature end of our sample substantially raised the velocity dispersion for cooler stars. Ages were calculated using dereddened *Gaia* $G_{BP} - G_{RP}$ color, however throughout this paper we show rotation periods as a function of effective temperature, T_{eff}. We chose to use T_{eff} as the abscissa because it is easier to divide stars into bins of roughly equal numbers in T_{eff}-space than in color-space.

The top panel of figure 3 shows the full McQuillan et al. (2014) sample (excluding visual binaries and subgiants) in grey, with coeval groups shown in color. The color of the points corresponds to the age ranges specified in the legend (in Gyr), which also apply to the lines

Fig. 3.— Top: rotation period vs effective temperature for stars in the McQuillan et al. (2014) catalog. The full catalog, with subgiants and visual binaries removed is shown in grey, and stars selected to be in different age groups (between 3500 and 5500 K) are overlayed in color. These age groups were selected using the Angus et al. (2019) gyrochronology relation. The legend in the center of the figure lists the age range, in Gyr, of each group. Bottom: velocity dispersion vs effective temperature for each age group. The color of the line corresponds to the color of the group shown in the top panel. If the gyrochronal model were correct at all ages, and the stars in each group were the same age across temperatures, the velocity dispersion would be constant as a function of $T_{\rm eff}$. However, the velocity dispersions of the oldest age groups increase with $T_{\rm eff}$, indicating the Angus et al. (2019) gyrochronology model underpredicts the the ages of late-K dwarfs relative to the ages of late G and early K dwarfs at old ages.

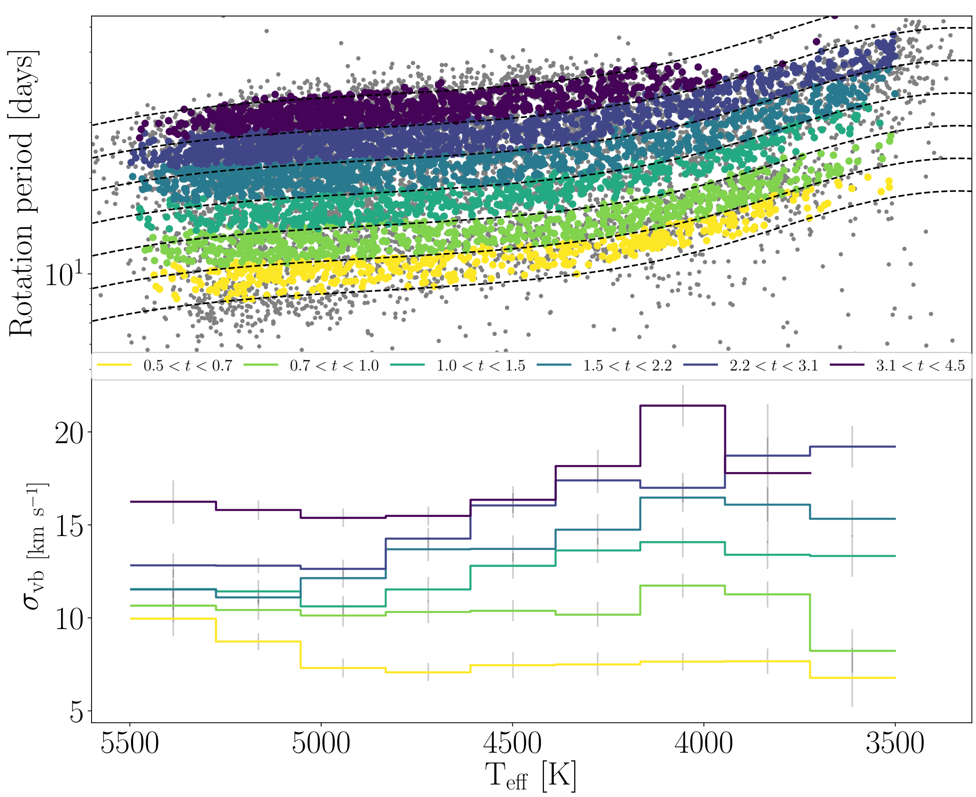

in the lower panel. The bottom panel shows the velocity dispersion, $\sigma_{v\mathbf{b}}$ of each age group, as a function of effective temperature. Overall, figure 3 shows that velocity dispersion increases with gyrochronal age across all temperatures, implying that both velocity dispersion and rotation periods increase with age as expected. The flat velocity dispersion of young stars as a function of temperature shows that the Praesepe-calibrated gyrochronology relation accurately predicts the relative ages of *young* field stars. If the gyrochronology relations worked at all ages and temperatures, the bottom panel of figure 3 would show a flat relationship between velocity dispersion and T_{eff}at all ages. However, velocity dispersion *increases* as a function of temperature for old stars, meaning the Angus et al. (2019) gyrochronology relation either under-predicts the ages of old, late-K dwarfs, or over-predicts the ages of old early-K and late-G dwarfs[2]. This suggests that the relationship between rotation period and photometric color or T_{eff} flattens out over time, and possibly even inverts. The lines of constant age (isochrones) sweeping diagonally upwards in the top panel of figure 3 are too steeply sloped at old ages.

3.2. The period-T_{eff} relations, revealed

Figure 4 shows rotation period vs. T_{eff} for our sample, coloured by ($v_{\mathbf{b}}$) velocity dispersion, where $\sigma_{v\mathbf{b}}$ was calculated for groups of stars over a grid in $\log_{10}$(period) and temperature. If we assume that mass dependent heating does not strongly affect this sample and $v_{\mathbf{b}}$ at low galactic latitudes is an unbiased tracer of $v_{\mathbf{z}}$, then $v_{\mathbf{b}}$ velocity dispersion can be interpreted as an age proxy and stars plotted in a similar color in figure 4 are similar ages. Interpreted this way, lines of constant age (isochrones) appear to follow the shape of the Praesepe-based gyrochronology model (black solid and dotted lines) at young ages. However, at older ages it appears that the relation between rotation period and T_{eff} flattens out, until eventually rotation period *decreases* with decreasing effective temperature at a given age.

The shape of the period-T_{eff} relations at old ages appears to follow the shape of the upper detection edge. The 'M dwarf dip' (van Saders et al. 2018), a feature of the McQuillan et al. (2014) rotation period catalog characterized by a dearth of slowly rotating M dwarfs between $\sim$2750 and 4250 K, is reflected in the lines of constant velocity dispersion (and presumed age) in the top panel of figure 4. If the shape of the upper edge of rotation period measurements is created by a detection limit, it could indicate the rotation periods at

[2]Since $v_{\mathbf{b}}$ velocity dispersion only provides relative and not absolute ages, it is difficult to tell whether the ages of cool stars are being under-predicted, the ages of hot stars being are over-predicted, or both.

Fig. 4.— Top: Rotation period vs effective temperature for stars in the McQuillan et al. (2014) sample, colored by the velocity dispersions of stars calculated over a grid in $\log_{10}$(period) and $T_{\rm eff}$. Bottom: the velocity dispersions of groups of stars, shown as a solid grid for clarity. The hatched area indicates the temperature regime where selection biases could play an important role, so these velocity dispersions should be interpreted with caution. The black solid lines on both panels show a 1.1 Gyr isochrone, calculated with the Angus et al. (2019) gyrochronology relation, which roughly traces the rotation period gap. The black dashed lines show a 650 Myr isochrone, indicating the location and shape of the Praesepe cluster (to which this gyrochronology model was calibrated). The black points show the 1.1 Gyr NGC 6811 open cluster.

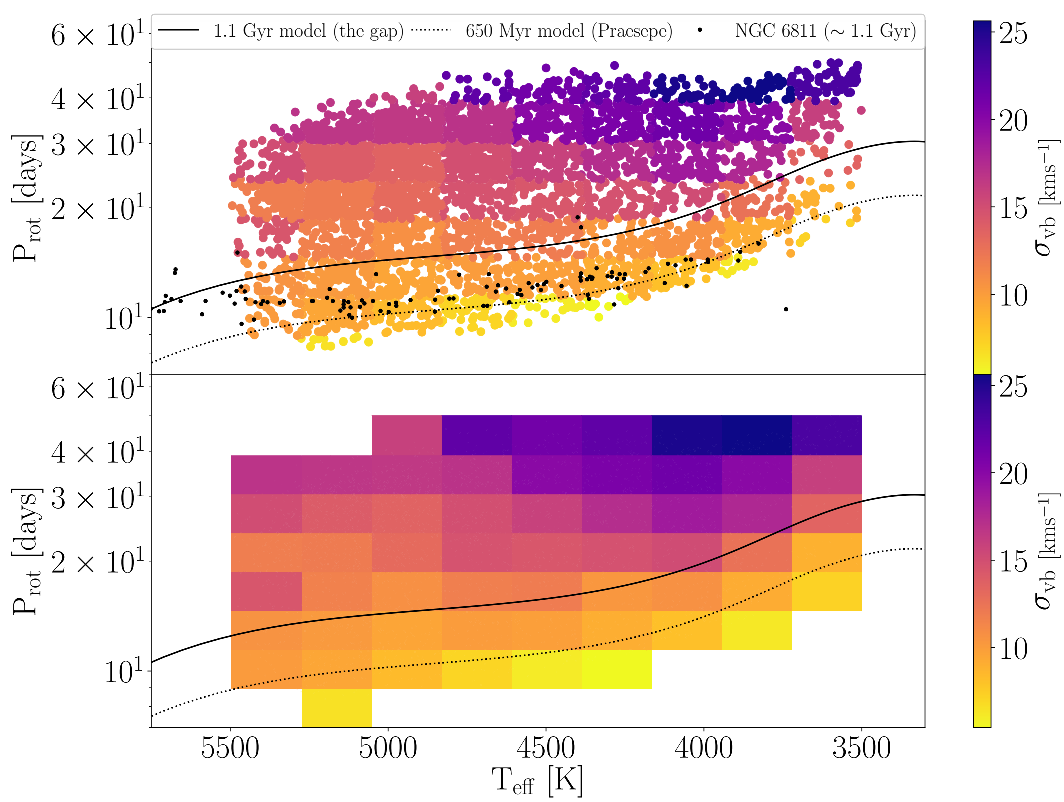

which stars of different temperatures become relatively inactive (and their rotation periods therefore become undetectable). If so, figure 4 suggests that stars cooler than $\sim$4500 K become inactive at a similar age, and stay active longer than stars hotter than $\sim$4500 on average.

The velocity dispersions of the coolest stars may be affected by a selection bias – these extremely faint stars are more difficult to detect at larger distances, larger heights above the plane, and therefore larger velocities. It is possible that some high velocity stars of temperatures cooler than $\sim$4000 K are missing from this sample, and the velocity dispersions may therefore appear lower than they truly are. This could be why the velocity dispersion appears to decrease towards the right of figure 4.

4. Discussion

4.1. The period gap

The origin of the rotation period gap, first identified by McQuillan et al. (2013) and visible in figures 3 and 4 still remains a mystery. This gap can be seen as an under-density of points between the 0.7-1.0 and 1.0-1.5 Gyr age ranges in figure 3 and roughly follows a line of constant gyrochronal age of around 1.1 Gyr (according to the gyrochronology relation of Angus et al. 2019), as shown in figure 4.

Several explanations for the gap's origin have been proposed, including a discontinuous star formation history (McQuillan et al. 2013; Davenport 2017; Davenport and Covey 2018), a rapid change in magnetic field structure (Reinhold et al. 2019), and erroneous rotation period measurements that are incorrect by a factor of two (Koen 2018). The latter explanation can be ruled out because stars below the gap have smaller velocity dispersions than the stars above the gap, indicating that they are kinematically younger (McQuillan et al. 2013; Davenport and Covey 2018), as evident in figures 3 and 4.

For stars below the gap, in the 0.7-1.0 Gyr age range shown in figure 3, velocity dispersion is relatively constant as a function of temperature, however above the gap, in the 1.0-1.5 Gyr age range and older, velocity dispersion increases with T_{eff}. The coolest stars in the 1.0-1.5 Gyr age range have the same velocity dispersion as the mid-temperature stars in the age range above, and the hottest stars in the age range above *that*, which indicates that the period-T_{eff} relations are *flat* at rotation periods between ∼15-25 days, for 5500 K $< T_{\mathrm{eff}} <$ 4000 K. Below the gap, velocity dispersion within a given period range appears to *decrease* with decreasing temperature. The opposite appears to be true above the gap.

The gap may be positioned at a significant Rossby number/age at which stellar magnetic dynamos go through a transition. Perhaps before the age of 1.1 Gyr, or at Rossby numbers less than ???, magnetic braking is more efficient for stars with deeper convection zones. Once stars reach this critical age or Rossby number their magnetic fields undergo some transition, which produces the gap in the rotation period-T_{eff} plane and after this transition, magnetic braking efficiency no longer increases with decreasing mass. Of course, it may be a coincidence that the gyrochronology relations seem to only flatten off above the period gap and we lack a sufficient quantity of data to do more than speculate here. New rotation periods from the *K2* and *TESS* missions may be able to validate or rule out this hypothesis in the future.

In the ∼ 1.1 Gyr NGC 6811 cluster, the rotation periods of mid-K dwarfs are faster than expected; their rotational evolution appears to have stalled, and they have similar rotation periods to the 650 Myr Praesepe cluster (Curtis et al. 2019). The rotation periods of the K dwarfs in NGC 6811 are plotted in figure 4. Although NGC 6811's G dwarfs fall on the 1.1 Gyr gyrochronology model, the K dwarfs lie only a little above the 0.65 Gyr gyrochronology model. NGC 6811 straddles the rotation period gap: its G dwarfs lie above it and its K dwarfs lie below it. This cluster may be the 'missing link' that connects two epoch of stellar spin-down. However, figure 3 indicates that the Praesepe gyrochronology model is, on average, a *good* model for stars younger than $\sim$1 Gyr suggesting that stars in the field follow the period-color/$T_{\rm eff}$ relation of Praesepe, at least up to around 1 Gyr. We do not see strong evidence of K dwarf stalling in the field.

5. Conclusion

We examined the gyrochronology relations using the velocity dispersions of field stars with measured rotation periods. We found that old groups of cool dwarfs selected to be coeval using the Angus et al. (2019) gyrochronology relation do *not* have the same velocity dispersion across all temperatures. This implies that the Angus et al. (2019) relation, which is based on the period-color relation of the 650 Myr Praesepe cluster, does not correctly describe the period-age-color/T_{eff} relation for old stars. It appears that the period-color/T_{eff} relation changes shape over time, *i.e.* the period-color/T_{eff} relation and the period-age relation are non-separable. At ages younger than $\sim$1 Gyr, rotation period is anti-correlated with T_{eff}: cooler stars spin more slowly than hotter stars of the same age. However, at old ages the opposite is true: cooler stars spin more rapidly than hotter stars of the same age. The period-color/T_{eff} relation appears to start flattening out after $\sim$1 Gyr (see figure 3), potentially around the same age, or just older than the period gap which is located at a gyrochronal age of around $\sim$1.1 Gyr (see figure 4). This gap may represent a significant transitional epoch in the magnetic behavior of stars. Finally, when velocity dispersion is interpreted as an age proxy, it appears that the oldest stars in the McQuillan et al. (2014) catalog are cooler than 4500 K, which suggests that lower-mass stars remain active for longer and their rotation periods can be measured at older ages. We outlined a number of scenarios which could provide alternative explainations for these observations, including incorrect dust corrections for the lowest-mass stars and an excess of companions increasing the velocity dispersion for these stars.

If the period-color/T_{eff} relation does invert at old ages as our results suggest, this would be a paradigm shift for gyrochronology. Stellar spin-down rate is thought to be directly tied to magnetic field strength, and the deeper convection zones of cooler stars generate stronger magnetic fields which *should* lead to more efficient angular momentum loss. However, the micro- and macro-physics of stellar structure and evolution and magnetic dynamo models are extremely complicated and a lot is still unknown about the magnetic behavior of stars. Observations like these can provide useful constraints for physical models, and may help to reveal new physical processes at work in stars like our own Sun and other planet hosts.

This work was partly developed at the 2019 KITP conference 'Better stars, better planets'. Parts of this project are based on ideas explored at the Gaia sprints at the Flatiron Institute in New York City, 2016 and MPIA, Heidelberg, 2017.

This work made use of the gaia-kepler.fun crossmatch database created by Megan Bedell.

Some of the data presented in this paper were obtained from the Mikulski Archive for Space Telescopes (MAST). STScI is operated by the Association of Universities for Research in Astronomy, Inc., under NASA contract NAS5-26555. Support for MAST for non-HST data is provided by the NASA Office of Space Science via grant NNX09AF08G and by other grants and contracts. This paper includes data collected by the Kepler mission. Funding for the *Kepler* mission is provided by the NASA Science Mission directorate.

This work has made use of data from the European Space Agency (ESA) mission *Gaia* (`https://www.cosmos.esa.int/gaia`), processed by the *Gaia* Data Processing and Analysis Consortium (DPAC, `https://www.cosmos.esa.int/web/gaia/dpac/consortium`). Funding for the DPAC has been provided by national institutions, in particular the institutions participating in the *Gaia* Multilateral Agreement.

REFERENCES

R. Angus, S. Aigrain, D. Foreman-Mackey, and A. McQuillan. Calibrating gyrochronology using Kepler asteroseismic targets. *MNRAS*, 450:1787–1798, June 2015. doi: 10.1093/mnras/stv423.

Ruth Angus et al. Towards precise stellar ages: combining isochrone fitting with empirical gyrochronology. *AJ*, 2019.

Astropy Collaboration, T. P. Robitaille, E. J. Tollerud, P. Greenfield, M. Droettboom, E. Bray, T. Aldcroft, M. Davis, A. Ginsburg, A. M. Price-Whelan, W. E. Kerzendorf, A. Conley, N. Crighton, K. Barbary, D. Muna, H. Ferguson, F. Grollier, M. M. Parikh, P. H. Nair, H. M. Unther, C. Deil, J. Woillez, S. Conseil, R. Kramer, J. E. H. Turner, L. Singer, R. Fox, B. A. Weaver, V. Zabalza, Z. I. Edwards, K. Azalee Bostroem, D. J. Burke, A. R. Casey, S. M. Crawford, N. Dencheva, J. Ely, T. Jenness, K. Labrie, P. L. Lim, F. Pierfederici, A. Pontzen, A. Ptak, B. Refsdal, M. Servillat, and O. Streicher. Astropy: A community Python package for astronomy. *A&A*, 558:A33, October 2013. doi: 10.1051/0004-6361/201322068.

M. Aumer and J. J. Binney. Kinematics and history of the solar neighbourhood revisited. *MNRAS*, 397:1286–1301, August 2009. doi: 10.1111/j.1365-2966.2009.15053.x.

Michael Aumer, James Binney, and Ralph Schönrich. Age-velocity dispersion relations and heating histories in disc galaxies. *MNRAS*, 462(2):1697–1713, Oct 2016. doi: 10.1093/mnras/stw1639.

S. A. Barnes. On the Rotational Evolution of Solar- and Late-Type Stars, Its Magnetic Origins, and the Possibility of Stellar Gyrochronology. *ApJ*, 586:464–479, March 2003. doi: 10.1086/367639.

S. A. Barnes. Ages for Illustrative Field Stars Using Gyrochronology: Viability, Limitations, and Errors. *ApJ*, 669:1167–1189, November 2007. doi: 10.1086/519295.

J. L. Curtis, M. A. Agüeros, S. T. Douglas, and S. Meibom. A Temporary Epoch of Stalled Spin-Down for Low-Mass Stars: Insights from NGC 6811 with Gaia and Kepler. *arXiv e-prints*, May 2019.

James R. A. Davenport. Rotating Stars from Kepler Observed with Gaia DR1. *ApJ*, 835(1):16, Jan 2017. doi: 10.3847/1538-4357/835/1/16.

James R. A. Davenport and Kevin R. Covey. Rotating Stars from Kepler Observed with Gaia DR2. *ApJ*, 868(2):151, Dec 2018. doi: 10.3847/1538-4357/aae842.

S. T. Douglas, M. A. Agüeros, K. R. Covey, and A. Kraus. Poking the Beehive from Space: K2 Rotation Periods for Praesepe. *ApJ*, 842:83, June 2017. doi: 10.3847/1538-4357/aa6e52.

Jacqueline K. Faherty, Adam J. Burgasser, Kelle L. Cruz, Michael M. Shara, Frederick M. Walter, and Christopher R. Gelino. The Brown Dwarf Kinematics Project I. Proper Motions and Tangential Velocities for a Large Sample of Late-Type M, L, and T Dwarfs. *AJ*, 137(1):1–18, Jan 2009. doi: 10.1088/0004-6256/137/1/1.

J. Holmberg, B. Nordström, and J. Andersen. The Geneva-Copenhagen survey of the Solar neighbourhood II. New uvby calibrations and rediscussion of stellar ages, the G dwarf problem, age-metallicity diagram, and heating mechanisms of the disk. *A&A*, 475: 519–537, November 2007. doi: 10.1051/0004-6361:20077221.

J. Holmberg, B. Nordström, and J. Andersen. The Geneva-Copenhagen survey of the solar neighbourhood. III. Improved distances, ages, and kinematics. *A&A*, 501:941–947, July 2009. doi: 10.1051/0004-6361/200811191.

Chris Koen. Modelling the rotation period distribution of M dwarfs in the Kepler field. *Ap&SS*, 363(1):11, Jan 2018. doi: 10.1007/s10509-017-3225-6.

Gregory M. Green. dustmaps: A Python interface for maps of interstellar dust. *The Journal of Open Source Software*, 3(26):695, Jun 2018. doi: 10.21105/joss.00695.

A. McQuillan, S. Aigrain, and T. Mazeh. Measuring the rotation period distribution of field M dwarfs with Kepler. *MNRAS*, 432(2):1203–1216, Jun 2013. doi: 10.1093/mnras/stt536.

A. McQuillan, T. Mazeh, and S. Aigrain. Rotation Periods of 34,030 Kepler Main-sequence Stars: The Full Autocorrelation Sample. *ApJS*, 211:24, April 2014. doi: 10.1088/0067-0049/211/2/24.

S. Meibom, S. A. Barnes, D. W. Latham, N. Batalha, W. J. Borucki, D. G. Koch, G. Basri, L. M. Walkowicz, K. A. Janes, J. Jenkins, J. Van Cleve, M. R. Haas, S. T. Bryson, A. K. Dupree, G. Furesz, A. H. Szentgyorgyi, L. A. Buchhave, B. D. Clarke, J. D. Twicken, and E. V. Quintana. The Kepler Cluster Study: Stellar Rotation in NGC 6811. *ApJ*, 733:L9, May 2011. doi: 10.1088/2041-8205/733/1/L9.

Travis S. Metcalfe and Ricky Egeland. Understanding the Limitations of Gyrochronology for Old Field Stars. *ApJ*, 871(1):39, Jan 2019. doi: 10.3847/1538-4357/aaf575.

B. Nordström, M. Mayor, J. Andersen, J. Holmberg, F. Pont, B. R. Jørgensen, E. H. Olsen, S. Udry, and N. Mowlavi. The Geneva-Copenhagen survey of the Solar neighbourhood. Ages, metallicities, and kinematic properties of 14 000 F and G dwarfs. *A&A*, 418:989–1019, May 2004. doi: 10.1051/0004-6361:20035959.

A. M. Price-Whelan, B. M. Sipőcz, H. M. Günther, P. L. Lim, S. M. Crawford, S. Conseil, D. L. Shupe, M. W. Craig, N. Dencheva, A. Ginsburg, J. T. VanderPlas, L. D. Bradley, D. Pérez-Suárez, M. de Val-Borro, (Primary Paper Contributors, T. L. Aldcroft, K. L. Cruz, T. P. Robitaille, E. J. Tollerud, (Astropy Coordination Committee, C. Ardelean, T. Babej, Y. P. Bach, M. Bachetti, A. V. Bakanov, S. P. Bamford, G. Barentsen, P. Barmby, A. Baumbach, K. L. Berry, F. Biscani, M. Boquien, K. A. Bostroem, L. G. Bouma, G. B. Brammer, E. M. Bray, H. Breytenbach, H. Buddelmeijer, D. J. Burke, G. Calderone, J. L. Cano Rodríguez, M. Cara, J. V. M. Cardoso, S. Cheedella, Y. Copin, L. Corrales, D. Crichton, D. D'Avella, C. Deil, É. Depagne, J. P. Dietrich, A. Donath, M. Droettboom, N. Earl, T. Erben, S. Fabbro, L. A. Ferreira, T. Finethy, R. T. Fox, L. H. Garrison, S. L. J. Gibbons, D. A. Goldstein, R. Gommers, J. P. Greco, P. Greenfield, A. M. Groener, F. Grollier, A. Hagen, P. Hirst, D. Homeier, A. J. Horton, G. Hosseinzadeh, L. Hu, J. S. Hunkeler, Ž. Ivezić, A. Jain, T. Jenness, G. Kanarek, S. Kendrew, N. S. Kern, W. E. Kerzendorf, A. Khvalko, J. King, D. Kirkby, A. M. Kulkarni, A. Kumar, A. Lee, D. Lenz, S. P. Littlefair, Z. Ma, D. M. Macleod, M. Mastropietro, C. McCully, S. Montagnac, B. M. Morris, M. Mueller, S. J. Mumford, D. Muna, N. A. Murphy, S. Nelson, G. H. Nguyen, J. P. Ninan, M. Nöthe, S. Ogaz, S. Oh, J. K. Parejko, N. Parley, S. Pascual, R. Patil, A. A. Patil, A. L. Plunkett, J. X. Prochaska, T. Rastogi, V. Reddy Janga, J. Sabater, P. Sakurikar, M. Seifert, L. E. Sherbert, H. Sherwood-Taylor, A. Y. Shih, J. Sick, M. T. Silbiger, S. Singanamalla, L. P. Singer, P. H. Sladen, K. A. Sooley, S. Sornarajah, O. Streicher, P. Teuben, S. W. Thomas, G. R. Tremblay, J. E. H. Turner, V. Terrón, M. H. van Kerkwijk, A. de la Vega, L. L. Watkins, B. A. Weaver, J. B. Whitmore, J. Woillez, V. Zabalza, and (Astropy Contributors. The Astropy Project: Building an Open-science Project and Status of the v2.0 Core Package. *AJ*, 156:123, September 2018. doi: 10.3847/1538-3881/aabc4f.

Adrian Price-Whelan. adrn/pyia: v0.2. Apr 2018. doi: 10.5281/zenodo.1228136.

L. M. Rebull, J. R. Stauffer, L. A. Hillenbrand, A. M. Cody, J. Bouvier, D. R. Soderblom, M. Pinsonneault, and L. Hebb. Rotation of Late-type Stars in Praesepe with K2. *ApJ*, 839:92, April 2017. doi: 10.3847/1538-4357/aa6aa4.

Timo Reinhold, Keaton J. Bell, James Kuszlewicz, Saskia Hekker, and Alexander I. Shapiro. Transition from spot to faculae domination. An alternate explanation for the dearth of intermediate Kepler rotation periods. *A&A*, 621:A21, Jan 2019. doi: 10.1051/0004-6361/201833754.

J. A. Sellwood. Secular evolution in disk galaxies. *Reviews of Modern Physics*, 86(1):1–46, Jan 2014. doi: 10.1103/RevModPhys.86.1.

A. Skumanich. Time Scales for CA II Emission Decay, Rotational Braking, and Lithium Depletion. *ApJ*, 171:565, February 1972. doi: 10.1086/151310.

J. L. van Saders, T. Ceillier, T. S. Metcalfe, V. Silva Aguirre, M. H. Pinsonneault, R. A. García, S. Mathur, and G. R. Davies. Weakened magnetic braking as the origin of anomalously rapid rotation in old field stars. *Nature*, 529:181–184, January 2016. doi: 10.1038/nature16168.

J. L. van Saders, M. H. Pinsonneault, and M. Barbieri. Forward Modeling of the Kepler Stellar Rotation Period Distribution: Interpreting Periods from Mixed and Biased Stellar Populations. *ArXiv e-prints*, March 2018.

This preprint was prepared with the AAS LaTeX macros v5.0.